

Transparent Ag-TiO₂-PMMA composite for optical limiting

XIAOYUN XU*

¹Guangzhou City University of Technology, Guangzhou 510800, China

²Key Laboratory of Polymer Processing Engineering of the Ministry of Education, South China University of Technology, Guangzhou 510641, China

The construction of the optical limiting materials is of great technological important for various applications such as in laser surgery, laser machining, optical communication and spectroscopy analysis. Despite of the great progress in development of optical non-linear materials, it still remains a great challenge for construction of optical limiting materials with combinative features of easy processing, strong optical limiting effect and broadband spectra response. Here we present the design and synthesis of the Ag-TiO₂-PMMA composite and characterization of its structure and optical properties. The composite is featured by the PMMA matrix embedded with the functional Ti-O structure units and Ag nanostructures. The composite is highly transparent and can be potentially shaped into various shapes. It presents broadband optical response covering the ultra-violet, visible and near-infrared waveband region from 200 to 750 nm. The nonlinear absorption coefficient of the composite is about 7 times higher compared with that of the pure PMMA. The application of the composite as optical limiting candidate is demonstrated and the optical limiting threshold of the composite reaches to 169.4 GW/cm². The results about the rational combination of the functional structure units in the composite provide valuable references for developing the next generation optical functional material.

(Received November 1, 2021; accepted February 10, 2022)

Keywords: Ag, TiO₂, PMMA, Transparent composite, Optical limiting

1. Introduction

Because of the increasing level of attention focused on the optical radiation shielding in laser surgery, laser machining, optical communication and spectroscopy analysis, there is rapidly growing requirement for non-linear optical materials with strong optical limiting activity. [1-5] Various types of nanostructured materials, such as CdS, CdTe, BN and Graphene, have been widely explored. [6-10] Benefited from the nano-size effect, the excellent non-linear optical response has been observed. Another types of material candidates are composites which are constructed by embedding functional low-dimensional nonlinear materials into the non-crystalline matrix. [11-14] This type of optical limiting materials has attracted increasing attention because it combines the advantages of robust performance of the nanostructures and easy fabrication feature of the non-crystalline matrix. Despite of the great progress in material synthesis, the category of the composite for optical limiting is still limited. Especially, few reports involve the success in construction of the composite embedded with high dielectric nanostructures although it is known that its highly polarized component

(e.g., Ti⁴⁺) is favorable for enhancing the non-linear optical properties.

In this letter, we report the success in fabrication of the Ag-TiO₂-PMMA composite with excellent non-linear optical properties. The composite shows broadband optical response feature in the whole ultra-violet, visible and near-infrared waveband region of 200-750 nm. The nonlinear absorption coefficient of the composite is about 7 times higher compared with that of the pure PMMA. The interesting optical properties are mainly contributed by the special Ag-TiO₂ composite configuration. The application of the composite as optical limiting candidate is demonstrated and the optical limiting threshold of the composite reaches to 169.4 GW/cm². The results indicate that the strategy of the rational combination of structure units provides an effective avenue for the development of functional photonic composite.

2. Experimental section

2.1. Material synthesis

The Ag-TiO₂-PMMA composite material system was

synthesized via sol-gel method. First, the PMMA solution was fabricated. In a typical synthesis procedure, 3.645 g polymethyl methacrylate (PMMA) was added into the 15 ml acetone and it was continuously stirred for 2 hours for dissolving PMMA. Second, the mixed solution composed of AgNO_3 and titanium n-propoxide was fabricated. For details, 0.005 g AgNO_3 powder was dissolved in 10 ml ethanol. Subsequently, 1 ml titanium n-propoxide was added into the solution drop by drop. The mixed solution was ultrasonically stirred for 20 minutes. Finally, the obtained PMMA solution and mixed AgNO_3 -titanium n-propoxide solution was homogeneously mixed and stirred for 1 hour. The resultant solution was transferred into silica-gel mold and kept for several days for drying. The resultant solid composite was obtained for further characterizations. The pure PMMA was also fabricated for comparison.

2.2. Material characterizations

The microstructures of the composite materials were characterized by using the high resolution transmission electron microscopy (TEM). It was carried out on a JEOL 2010F transmission electron microscope. The absorption features of the composite materials were analyzed by optical absorption spectrum which was performed on the Lambda 900 UV/VIS/NIR spectrometer. The operation wavelength is 200-800 nm. The luminescence properties of the samples were studied with an FLS920 fluorescence spectrometer (Edinburgh Instrument Ltd., Edinburgh, UK). For investing the luminescence properties, the excitation and luminescence spectra were measured and analyzed. The excitation source is the xenon lamp with the power of 450 W. The optical limiting properties of the samples were studied via employing a classic open-aperture Z-scan experiment setup. The laser source is a Coherent femtosecond laser with the wavelength, pulse-duration and repetition rate of 800 nm, 120 fs and 1kHz, respectively.

3. Results and discussion

Fig. 1(a) and (b) shows the photos of the resultant pure PMMA and Ag-TiO₂-PMMA solution, respectively. Both of the solutions are homogeneously and clearly. After kept at room temperature for 7 days, the pure PMMA and Ag-TiO₂-PMMA can be obtained. As exhibited in Fig. 1(c) and (d), both samples are highly transparent. The Ag-TiO₂-PMMA sample shows a slight yellow color and it is different from the pure PMMA which is totally colorless. The sample can also be fabricated into homogeneous film.

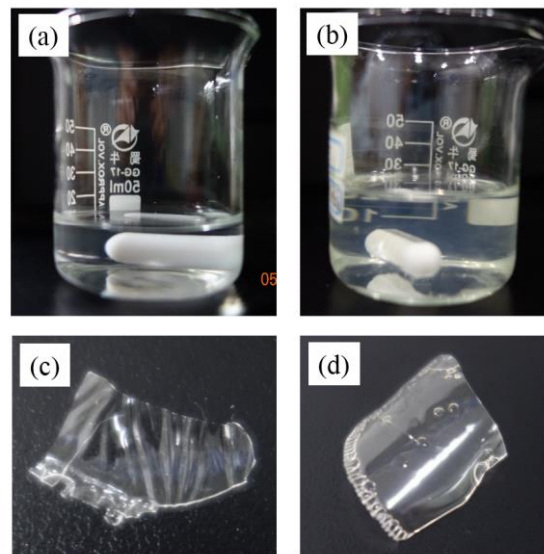


Fig. 1. (a-d) The photos of the synthesized PMMA solution (a), Ag-TiO₂-PMMA composite derived solution (b), pure PMMA (c), and Ag-TiO₂-PMMA composite (d)

The optical absorption properties of the samples were studied. Fig. 2a shows the absorption spectrum of the pure PMMA and onset of the absorption is at ~318 nm. A sharp absorption band at ~277 nm can be ascribed to the characteristic absorption of the host matrix. The results indicate that the pure PMMA exhibits excellent optical transmission in the whole visible waveband. Fig. 2b shows the absorption spectrum of the Ag-TiO₂-PMMA composite sample. It can be observed that the addition of Ag and TiO₂ leads to the notable change in the absorption feature in both of the ultra-violet and visible waveband. On one hand, the absorption in the ultra-violet waveband is strongly increased and absorption onset shifts to ~380 nm. This can be ascribed to the valence-conduction band transition of semiconductor TiO₂. On the other hand, the broadband absorption in the visible waveband also appears. This might be originated from the Ag nanostructures, such as Ag particles, dimers and other complicate configurations. To confirm this origin, the microstructures of the composite sample were characterized by TEM and some tiny nanoparticles can be observed. The inset of Fig. 2(b) shows a typical TEM image of the composite. The lattice spacing was calculated to be ~0.1455 nm, which is well consistent with the (220) plane of crystalline Ag. The results confirm the precipitation of Ag nanoparticle inside the Ag-TiO₂-PMMA composite. Interestingly, the color of the composite gradually become dark with the extension of the holding time of the composite, hinting that the microstructure of the composite always changes. About the physical mechanism, it was supposed that the formation of Ag is associated with the TiO₂-mediated photoreduction of Ag ion into Ag nanoparticles. It can be confirmed by the holding duration dependent color change and it was found that the color change can be well prevented in dark environment.

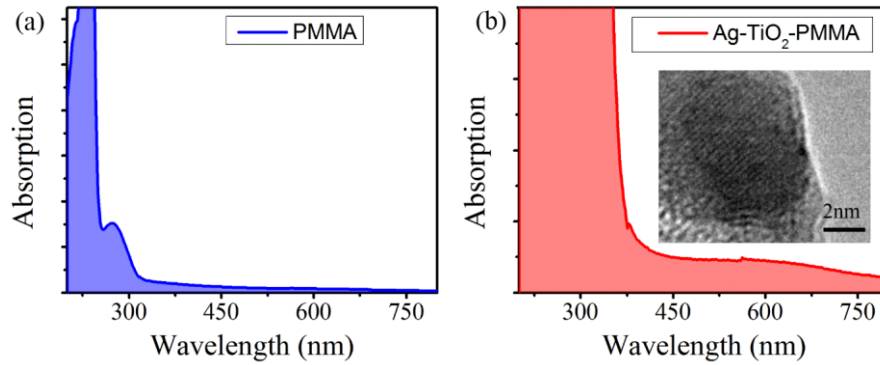


Fig. 2. The absorption spectra of the pure PMMA (a) and Ag-TiO₂-PMMA composite (b). The inset of Fig. 2(b) is the high-resolution TEM image of the Ag-TiO₂-PMMA composite (color online)

The luminescent properties of the pure PMMA and the Ag-TiO₂-PMMA composite were studied. No obvious luminescence can be observed in pure PMMA sample. Interestingly, intense visible luminescence can be observed in the Ag-TiO₂-PMMA composite. Fig. 3(a) presents the corresponding steady excitation and luminescence spectra. Under excitation with 396 nm, the luminescence spectrum is characterized by an intense luminescence band with the central wavelength at ~550 nm. By tuning the excitation wavelength to 466 nm, the luminescence spectrum is characterized by two broad bands with the central wavelength at 550 and 725 nm and the intensity of two emission bands are comparable. According to previous studies, the luminescence bands at green and red

wavebands can be ascribed to the radiative electronic transition of distinct Ag related clusters (e.g., Ag₃^{m+} and Ag₆ⁿ⁺) [15-17]. The luminescence dynamics were also studied and the decay curves were fitted. The decay curves are exhibited in Fig. 3(b) and the fitting results are shown in Table 1 and 2. The results show that the luminescence band at 550 nm can be fitted into two different dynamics and the decay lifetimes are estimated to be ~13.6 and 1.5 μs. For the luminescence band at 725 nm, it can also be fitted into two different dynamic process. The average lifetimes are estimated to be ~17.3 and 1.5 μs. Above results indicate that the radiative transitions are originated from the different active centers.

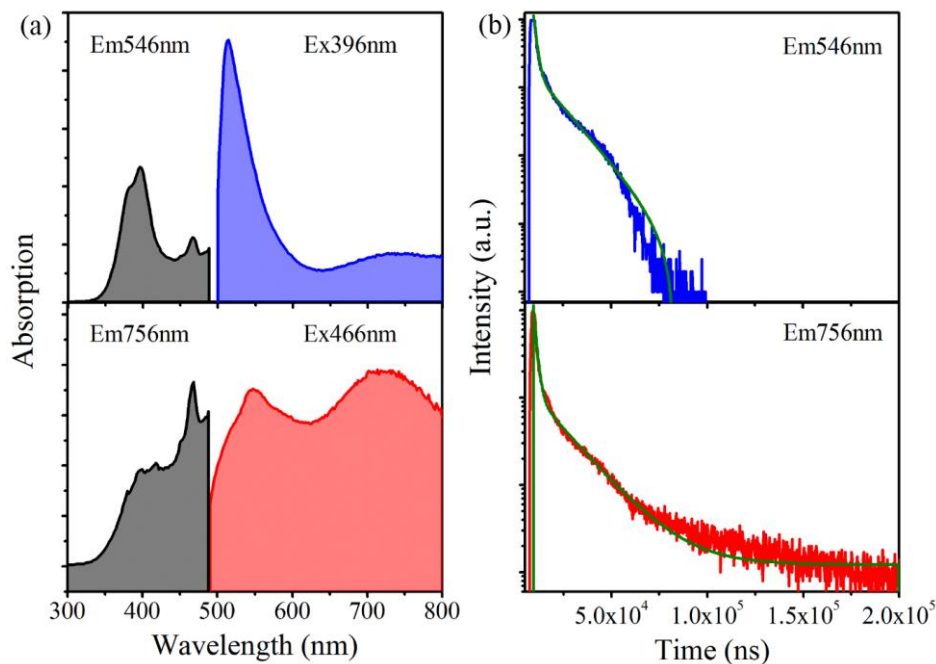


Fig. 3. (a) The excitation and luminescence spectra of Ag-TiO₂-PMMA. (b) The luminescence decay of Ag-TiO₂-PMMA composite at 546 and 756 nm (color online)

Table 1. The exponential fitting of the luminescence decay of Ag-TiO₂-PMMA at 546nm

Model	ExpDecay1		
Equation	$y=y_0+A_1*\exp(-(x-x_0)/t_1)+A_2*\exp(-(x-x_0)/t_2)$		
Reduced Chi-Sqr	17146.72022		
Adj.-Square	0.98865		
		Value	Standard Error
EM546	y0	-7.62919	10.83498
EM546	x0	9700.27476	
EM546	A1	1616.85184	
EM546	t1	13574.97693	798.8842
EM546	A2	9135.5962	
EM546	t2	1520.26092	32.29842

Table 2. The exponential fitting of the luminescence decay of Ag-TiO₂-PMMA composite at 756 nm

Model	ExpDecay1		
Equation	$y=y_0+A_1*\exp(-(x-x_0)/t_1)+A_2*\exp(-(x-x_0)/t_2)$		
Reduced Chi-Sqr	3.43746		
Adj.-Square	0.9811		
		Value	Standard Error
EM756	y0	12.2753	0.29667
EM756	x0	7825.66428	2.80039E8
EM756	A1	25559.78186	3.18522E10
EM756	t1	1513.76519	17.42326
EM756	A2	1173.97059	1.27898E8
EM756	t2	17315.43075	177.11998

The non-linear optical properties were studied by the classic Z-scan method. A focused 120 femtosecond laser beam with the wavelength of 800 nm and repetition rate of 1 kHz was employed as the investigated light. The sample was moved in a three-dimensional translation stage in the vicinity of the focus point. The power density can be tuned via changing the size of the focused beam. As a result, the power density dependent optical transmittance can be achieved. Fig. 4(a) and (b) compare the open aperture Z-scan curves of the pure PMMA and the Ag-TiO₂-PMMA composite. Under excitation with the ultra-short pulse, the Z-position dependent normalized transmittance in both samples show the valley profiles, indicating the reverse saturable absorption properties. The transmittance

becomes lower with the increase of the input laser intensity, demonstrating the existence of the optical limiting effect. Notably, under the same power intensity, the valley in the Ag-TiO₂-PMMA composite is broader and deeper compared with that of the pure PMMA. Particularly, under the laser irradiation with the power intensity of 500 μ W, the normalized transmittance of the Ag-TiO₂-PMMA composite reaches to ~ 0.14 , which is much lower than ~ 0.71 in the pure PMMA. The results firmly demonstrate the excellent optical limiting performance of the Ag-TiO₂-PMMA composite.

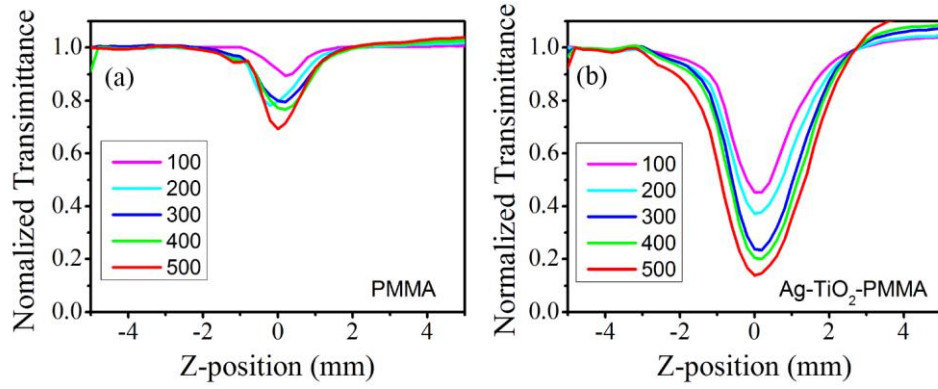


Fig. 4. (a) The open aperture Z-scan curves of PMMA. (b) The open aperture Z-scan curves of PMMA (color online)

The results were further analyzed based on the nonlinear light-matter interaction. According to the classic non-linear optics theory, the optical-path dependent transmittance can be described by using the following relation:

$$T(Z) = \sum_{m=0}^{\infty} \frac{[-q_0(Z)]^m}{(m+1)^{1.5}} \quad (1)$$

$$q_0 = \beta \frac{I_0 [1 - \exp(-\alpha_0 L)]}{\left[1 + \left(\frac{Z}{Z_0}\right)^2\right] \alpha_0} \quad (2)$$

$$\beta = \beta_0 / \left(1 + \frac{I}{I_{sat}}\right) \quad (3)$$

where Z is the location of the tested sample, α_0 is the linear absorption coefficient, β is the nonlinear absorption coefficient, Z_0 is the diffraction length of the optical beam,

β_0 is coefficient under low irradiance condition, and I_{sat} is saturation irradiance of non-linear absorption. Based on above relations, the critical parameter β which indicates the non-linear property of the sample can be estimated and the results are presented in Fig. 5a. Significantly, the β value of the Ag-TiO₂-PMMA composite is 7 times higher compared with that of the pure PMMA. This can be ascribed to the enhanced nonlinear light-matter interaction in the Ag-TiO₂-PMMA composite. With the increase of the input light intensity, the β value of both samples gradually decreases, probably associated with the non-linear saturation absorption effect. Additionally, the I_{sat} can also be obtained by fitting according to the relation (3) and the results are shown in Table 3. The I_{sat} of the Ag-TiO₂-PMMA composite was calculated to be ~ 154 GW/cm², which is larger than that of the pure PMMA (96.6 GW/cm²). The results further confirm the strong non-linear absorption properties of the Ag-TiO₂-PMMA composite.

Table 3. The two-photon absorption fitting for the sample of Ag-TiO₂-PMMA at 800 nm

Model	Function		
Equation	beta0(1+x/lsat)		
Reduced Chi-Sqr	3.25553E-7	6.5785E-5	
	0.99702	0.98618	
Adj.-Square		Value	Standard Error
PMMA	beta0	0.06969	0.00217
PMMA	lasat	96.57125	5.8308
Ag-TiO ₂ -PMMA	beta0	0.46811	0.02114
Ag-TiO ₂ -PMMA	lasat	154.00485	16.19274

The interesting non-linear optical response features of the constructed materials invites us to explore its application for optical limiting. To test it, the input power density dependent transmittance was measured the results

are presented in Fig. 5b. The optical transmittance of both samples decreases when the power density of the input light reaches to a certain value. Notably, it can be directly observed that the optical limiting performance of the

Ag-TiO₂-PMMA composite is superior compared with that of the pure PMMA. The optical limiting threshold can be used to indicate the optical performance. It can be defined as the intensity of the input light when the transmittance reaches to 50%. According to Fig. 5b, the optical limiting threshold of the Ag-TiO₂-PMMA composite was calculated to be 169.4 GW/cm². In stark contrast, no obvious optical limiting threshold can be observed in pure PMMA. The physical mechanism behind the excellent optical limiting performance can be further discussed based on the microstructure of the composite system. On one hand, Ti-O structure units embedded inside the

composite contribute to the strong absorption in the waveband region of less than 380 nm through valance-conduction band electronic transition. On the other hand, the Ag nanostructures inside the composite help to generate broadband surface plasmonic resonating in the waveband region of 380-750 nm. These unique structures are supposed to cooperatively lead to the strong optical limiting performance. Furthermore, because the Ag-TiO₂-PMMA composite presents broadband absorption feature, the optical limiting function can be expected to act in other wavebands beyond the 800 nm.

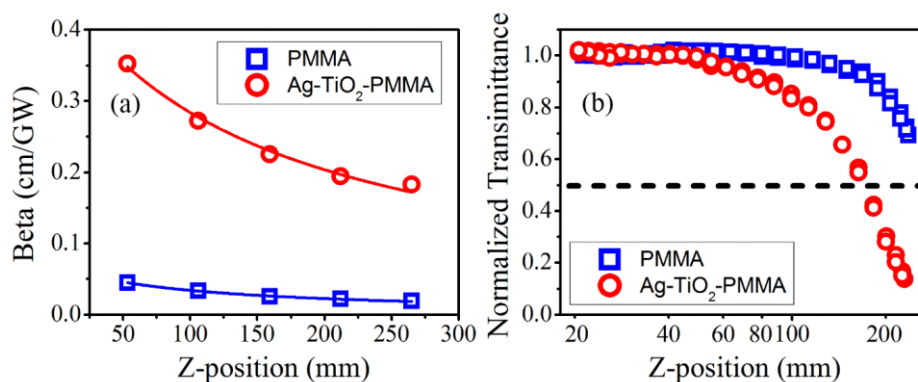


Fig. 5. The on-focus power density dependent lowest transmission of the pure PMMA and Ag-TiO₂-PMMA composite (color online)

4. Conclusions

In summary, we have proposed the design and fabrication of the Ag-TiO₂-PMMA composite with excellent non-linear optical properties. The nonlinear absorption coefficient of the composite is about 7 times higher compared with that of the pure PMMA. The application of the composite as optical limiting candidate has been demonstrated and the optical limiting threshold of the composite reaches to 169.4 GW/cm². In addition, benefiting from the broadband optical absorption feature of the composite, the composite can be further elaborated into the novel broadband optical limiting device. Furthermore, the finding about the collaborative effects of various functional units in the composite provides valuable clues for developing the next generation optical functional material by rational tuning the microstructures of the composite.

Acknowledgments

We gratefully acknowledge the financial support from National Natural Science Foundation of China (12104163), the Department of Education of Guangdong Province (2020KTSCX202), the Fund for Art & Design in Guangzhou City University of Technology (60-CQ190025)

and the Open Fund of Key Laboratory of Electromagnetic Transformation and Detection (Luoyang Normal University).

References

- [1] M. Scalora, J. P. Dowling, C. M. Bowden, M. J. Bloemer, *Phys. Rev. Lett.* **73**, 1368 (1994).
- [2] M. Feng, H. Zhan, Y. Chen, *Appl. Phys. Lett.* **96**, 033107 (2010).
- [3] N. Mackiewicz, T. Bark, B. Cao, J. A. Delaire, D. Riehl, W. L. Ling, S. Foillard, E. Doris, *Carbon* **49**, 3998 (2011).
- [4] D. Dini, M. J. F. Calvete, M. Hanack, *Chem. Rev.* **116**, 13043 (2016).
- [5] Y. Zhu, Y. Kang, Z. Gu, J. Zhang, *Adv. Opt. Mater.* **9**, 2002072 (2021).
- [6] M. Stavrou, I. Papadakis, S. Bawari, T. N. Narayanan, S. Couris, *J. Phys. Chem. C* **125**, 16075 (2021).
- [7] N. Venkatram, D. N. Rao, *Opt. Express* **13**, 867 (2005).
- [8] G. He, Q. Zheng, K. Yong, A. I. Rysanyanskiy, P. N. Prasad, A. Urbas, *Adv. Phys. Lett.* **90**, 181108 (2007).
- [9] S. J. Varma, J. Kumar, Y. Liu, K. Layne, J. Wu, C. Liang, Y. Nakanishi, A. Aliyan, W. Yang, P. M. Ajayan, J. Thomas, *Adv. Opt. Mater.* **5**, 1700713

- (2017).
- [10] B. A. Unlu, A. Karatay, E. A. Yildiz, M. L. Yola, M. Yuksek, N. Atar, A. Elmali, *Opt. Mater.* **121**, 111630 (2021).
- [11] R. Zieba, C. Desroches, F. Chaput, M. Carlsson, B. Eliasson, C. Lopes, M. Lindgren, S. Parola, *Adv. Funct. Mater.* **19**, 235 (2009).
- [12] X. Zheng, M. Feng, H. Zhan, *J. Mater. Chem. C* **1**, 6759 (2013).
- [13] Z. Shi, N. Dong, D. Zhang, X. Jiang, G. Du, S. Lv, J. Chen, J. Wang, S. Zhou, *J. Am. Ceram. Soc.* **102**, 3965 (2019).
- [14] X. Feng, Z. Shi, J. Chen, T. Yu, X. Jiang, G. Du, J. Qiu, S. Zhou, *Adv. Opt. Mater.* **8**, 1902143 (2020).
- [15] A. Simo, J. Polte, N. Pfänder, U. Vainio, F. Emmerling, K. Rademann, *J. Am. Chem. Soc.* **134**, 18824 (2012).
- [16] L. A. Peyser, A. E. Vinson, A. P. Bartko, R. M. Dickson, *Science* **291**, 103 (2001).
- [17] D. Grandjean, E. Coutiño-Gonzalez, N. T. Cuong, E. Fron, W. Baekelant, S. Aghakhani, P. Schlexer, F. D'Acapito, D. Banerjee, M. B. J. Roeffaers, M. T. Nguyen, J. Hofkens, P. Lievens, *Science* **361**, 686 (2018).

*Corresponding author: xuxiaoyun@gcu.edu.cn